Design and Experiment of a Wheel Precision Seed-Metering Device with Cells for Corn

Kezhou CHEN, Xing LIU, Xin HE, Xun WANG, Yanzhi LIU, Wei LI*

Abstract: In this study, a wheel seed-metering device with cells for corn was built to enhance seed-metering performance and shorten the design cycle. The actual seed-metering process was analyzed and the three main factors influencing seed metering were obtained: rotational speed of the seed-metering device, hole diameter, and hole pitch. With the three factors as the test factors, and the QFI, MISS and MULT index as the test indexes, the multiple quadratic rotation orthogonal combination test was carried out. Using *Design-Expert 8.0.6* to analyze the test data, the mathematical model between the test factors and the test index was obtained. The parameter optimization results indicate that optimal performance of the seed-metering device can be achieved under a rotational speed of 30.32 rpm, hole diameter of 13 mm, and hole pitch of 45 mm, qualification rate, miss-seeding rate, and reseeding rate were 94.99%, 1.93%, and 3.08%, respectively. Under the optimal parameter combination, the field test proved that the qualification rate, miss-seeding rate, and reseeding rate were 91.81%, 3.08%, and 5.11%, respectively. The test results were close to the optimization results, which could show the agronomic requirements of the precision sowing of maize.

Keywords: Box-Behnken design; performance test; response surface methodology; seed-metering device

1 INTRODUCTION

Corn is one of three major grain crops in China suitable for precision sowing. Precision seeding techniques can increase both corn yields and revenues [1, 2]. In precision sowing, the seed metering device is a key component and its performance will have a direct impact on crop quality and labor costs [3-5]. In this context, development and improvement of seed metering devices depend on convenient and rapid detection of several performance indices, including qualified, miss-seeding, and miss-filling rates [6-8].
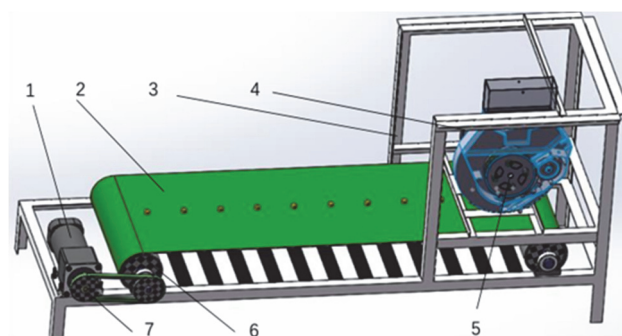
At present, precision seed-metering devices commonly used in China include the horizontal disc, inclined disc, cell wheel, composite seed-filling, and pneumatic types. According to working principles, seed-metering devices can be classified as either mechanical or pneumatic [9-12]. Pneumatic seed-metering devices are highly adaptive and can be universally applied since there are no strict requirements for seed shape or dimensions; however, shortcomings include complex structures, high processing costs, and frequent failures [13]. In contrast, mechanical seed-metering devices are characterized by a simple structure and stable performance, and are easy to repair. Therefore, small mechanical precision seeders are the most prevalent precision seed-metering devices in China [14]. Due to the high cost and huge size of existing seed-metering devices, small-scale experimental platforms provide the best way to optimize the quality and speed of precision seed-metering [15, 16].

The study completed the construction of the device through the design of the key components of the cell-wheel corn precision seed-metering device. Through the analysis of the actual seed-metering process, the factors influencing seed metering were obtained. Furthermore, seed-metering performance tests were performed, working parameters of the seed-metering device were optimized and then the field tests were conducted to validate the results.

2 MATERIALS AND METHODS
2.1 Design of the Complete Machine

The cell wheel precision seed-metering device is comprised of a platform, seed-metering device, seed-metering device motor, transmission device, transmission device motor, belt, roller, and detection and control devices, as shown in Fig. 1. The seed-metering device was installed above the transmission device and on the right side of the platform. The motor driving the seed-metering device was mounted on the right side of the seed-metering device. The transmission device, located below the seed-metering device, was fixed to the bottom of the device via two rollers. Another motor, used to drive the transmission device via a belt, was placed on the bottom left side of the device. To ensure the reliability of the platform in service, the motor driving the transmission device was hinged on one side with the platform, and connected on the other side using long bolts, thus allowing the belt to be conveniently fastened when necessary.

Figure 1 Cell wheel precision seed-metering device
1. Motor driving transmission device; 2. Transmission device; 3. Platform; 4. Motor driving seed-metering device; 5. Seed-metering device; 6. Roller; 7. Belt

After the power is switched on, the motor powers the seed-metering device through direct coupling, while the other motor drives the transmission device via the belt. Seeds in the tank first fall into the seed-metering device, and are then transferred to the transmission device. Movement of the transmission device relative to the seed-metering device simulates movement of the seed-metering device in the field. Tachometers were used to monitor real-

time speeds of the seed-metering device and the transmission device and the driving motors were used to match the working speeds, thereby simulating the entire seed-metering process. By recording the entire process and performing statistics on the qualified rate, reseeding rate, and miss-filling rate, seed metering-related indices of the cell wheel-type seed-metering device were obtained at different speeds, which provide a basis for design and optimization of the seed-metering device, as shown in Fig. 2.
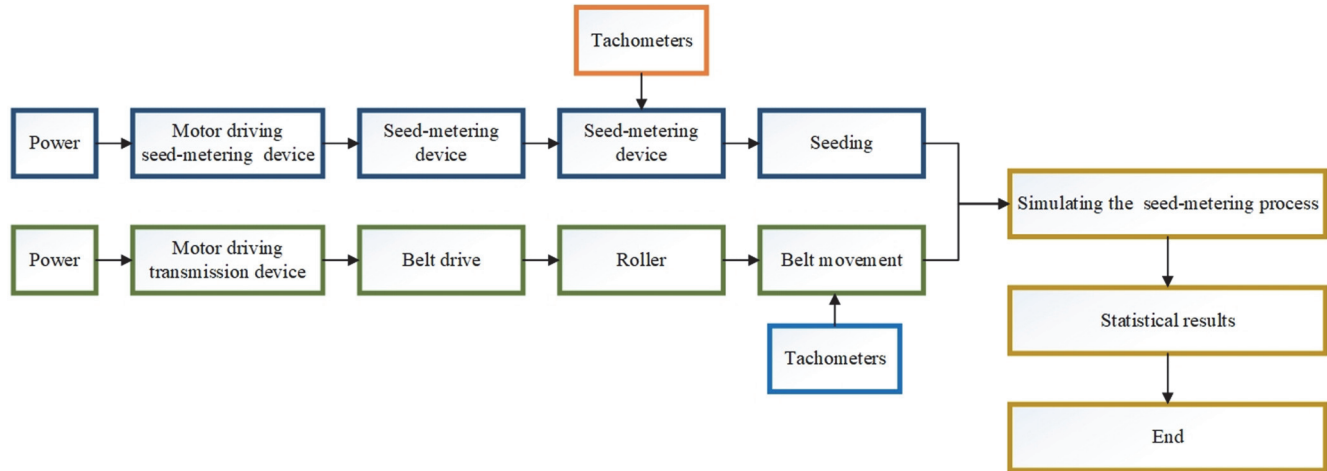
2.2 Design of Key Parts
2.2.1 Seed-Metering Device

The cell wheel diameter is directly related to the overall size of the seed-metering device, linear speed of the cell wheel, centripetal force required to move the seeds, and other parameters [17, 18]. In relation to the cell wheel diameter, the following simultaneous equations can be established:

Figure 2 Working principles of cell wheel precision seed-metering device

$$S_{M,N} = (M-1)(N-1)bl \tag{1}$$

$$v_w = \frac{\pi D n}{60} \tag{2}$$

$$D = \frac{zlv_w}{\pi v_m} \tag{3}$$

where $S_{M,N}$ denotes the number of plants per hectare, plants/ha; M denotes the number of rows; N denotes the number of columns; b denotes the row spacing, (m); l denotes the plant spacing, (m); n is the rotational speed of the cell wheel, rpm; v_w is the linear speed of the cell wheel, (m/s); D is the cell wheel diameter, m; z represents the hole count of the cell wheel; and v_m is the working speed of the seeder (m/s).

Specifically, the corn set of plants per hectare must be higher than 75000 plants/ha. Considering a row spacing of 0.5 m and an approximately square plot *(M = N)*, when $M > 273$, the required planting density is satisfied, i.e., $l < 0.027$. In our test, we set $l = 0.2$ m, such that, $S_{M,N} = 99630$ plants/ha.

Combining Eqs. (2) and (3) yields

$$z = \frac{60 v_m}{ln} \tag{4}$$

In general, the cell wheel rotational speed n is 30-40 rpm, and the seeder working speed v_m is 1-2 m/s, therefore, the cell wheel hole count z was set to 12. The cell wheel diameter D was 0.14 m.

The hole parameters are key design parameters that directly affect the seed filling, seed carrying, and seed charging processes of the seed-metering device and overall performance of the device [19]. In our design, the types holes are hemispherical. For precision sowing, the outline dimensions of corn seeds were measured and the mode of successful entry of the seeds into the holes was analyzed to ensure only one seed enters each hole.

Zhengdan 958 coated corn seeds from Henan Province were measured and assumed to approximately trapezoidal with upper base length $d_l = 8.32$ mm, lower base length $d_w = 3.04$ mm, height $h = 10.15$ mm, and thickness $t = 5.47$ mm. Seeds can enter holes in one of two positions: flat-lying posture and side-lying posture. Limit analysis was performed on the two postures using the measured seed dimensions, as shown in Fig. 3.
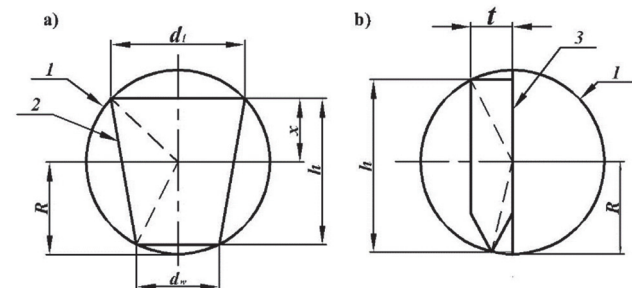

Figure 3 Relationship between hole diameter and flat-lying posture
1. Hole; 2. Seed flat-lying posture; 3. Seed side-lying posture.
d_l is the upper base length, mm; d_w is the lower base length, mm; t is the seed thickness, mm; h is the seed height, mm; R is the hole radius, mm; X is the distance from upper base to hole center, mm.

Fig. 3a shows the minimum hole diameter when seeds enter holes in the flat-lying posture. In this case, the

relationship between hole diameter and seed dimension can be expressed as:

$$R = \sqrt{\left(\frac{d_l}{2}\right)^2 + x^2} = \sqrt{\left(\frac{d_w}{2}\right)^2 + (h-x)^2} \qquad (5)$$

According to Eq. (5), when seeds are in the flat-lying posture, the minimum hole radius is 6 mm; that is, the minimum hole diameter is 12 mm.

Fig. 3b shows the maximum hole diameter when seeds enter holes in the side-lying posture. In this case, the relationship between hole diameter and seed dimension can be expressed as

$$h - \sqrt{R^2 + \left(\frac{t}{2}\right)^2} = \sqrt{R^2 + t^2} \qquad (6)$$

According to Eq. (6), when seeds are in the flat-lying posture, the maximum hole radius is 6.79 mm; that is, the maximum hole diameter is 14 mm.

Based on the above analysis, to ensure only one seed enters each hole, the hole diameter should be 12 mm $< d <$ 14 mm.

Working requirements for the seed-metering device are as follows: At a working speed of 7-10 km/h, the seed-metering device should be able to perform precision seed-metering with a plant spacing of 200 mm. A 12-hole cell wheel seed-metering device was adopted to develop the device.

The rotational speed V_s of the seed-metering device is:

$$V_s = \frac{k + l}{zl} \qquad (7)$$

where V_s denotes the rotational speed of the seed-metering device, rpm; z is the hole count of the seed plate; k is the working speed of the seed-metering device (7-10 km/h), rpm; l denotes the spacing of corn plants, mm.

At the highest speed of 10 km/h, the rotational speed of the seed plate is 37.9 rpm. The driving motor of the seed-metering device is directly connected to the seed-metering device, therefore, the rotational speed of the seed-metering device is equal to the rotational speed of the motor. To guarantee a certain allowance, a maximum possible rotational speed of 50 rpm was set. To achieve this, a *5IK120RGN-CF* motor with a rated power of 120 W and maximum rotational speed of 54 rpm was selected.

2.2.2 Conveying Mechanism

When ejected from the cell wheel seed-metering device, corn seeds have high kinetic energy. To make sure seeds land on the conveying belt with only a small rebound and without rolling, and to ensure a reliable and stable conveying process, a conveying belt composed of PVC conveyor and plush fabric was selected as the transmission device of the device. As a specialized transmission device, the PVC conveyor ensures precision and reliability. The plush fabric provides excellent shock absorption and reliably ensures seeds land in the desired position with only

a small amount of rebound and without rolling. In addition, to ensure there are more than five seeds on the conveying belt surface, dimensions of the PVC conveyor and the plush fabric were designed as follows: total conveyor length of 2600 mm; conveyor width of 400 mm; conveyor thickness of 2 mm; plush fabric perimeter of 2600 mm; plush fabric width of 300 mm.

Due to the frequent start/stop nature and high rotational speed of the conveying belt, a servo motor was selected to drive the transmission device [20]. The rotational speed n of the conveying roller is:

$$n = \frac{V_t}{\pi D} \qquad (8)$$

where n denotes the rotational speed of the roller, rpm; V_t denotes the speed of the transmission device, set as 7-10 km/h; and D is the diameter of the roller, set as 114 mm. Based on the highest speed of the transmission device of 10 km/h, the rolling speed is 465.6 rpm. The conveying wheel has a transmission ratio of 1:1, therefore, the rotational speed of the roller is equal to the rotational speed of the conveying belt motor. To guarantee a certain allowance, the motor was set to the highest rotational speed of 500 rpm. Thus, the *5IK120RGN-CF* motor with a rated power of 120 W was selected.

2.2.3 Detection Device

The sensor detection device is used to detect the speed of the transmission device and the rotational speed of the seed-metering device. The speed of the transmission device is equivalent to the speed of the advancing seed-metering device. Each time the seed-metering device makes one full rotation, 12 piles of seeds are ejected. Once the seeding speed of the seed-metering device is determined, a pile spacing of 200 mm is adopted to calculate the rotational speed. For simplicity and convenience, *RC41B* digital tachometer revolution meters was adopted and used in combination with the *U-groove L-type* optoelectronic switches for detection [21, 22].

2.3 Experimental Details

The proposed cell wheel seed-metering device for corn was tested in accordance with the Testing methods of single seed drills (precision drills) *(GB/T 6973-2005)* with rotational speed of the seed-metering device, hole diameter of the seed plate, and hole pitch of the seed plate as the independent variables. Response values were the qualification index, miss-seeding index, and reseeding index [23-25]. The test was carried out in the Agricultural Machinery Laboratory of Northwest Agriculture & Forestry University using a self-made cell wheel precision seed-metering device, as shown in Fig. 4. *Zhengdan 958* seeds with uniform dimensions and capable of adapting to the hole size of the seed plate were used as the test material to minimize the influence of seed dimensions on the results.

Considering the structural limitations of the seed-metering device and the factors influencing the actual seed metering process, the main influencing factors were identified as rotational speed of the seed-metering device, hole diameter of the seed plate, and hole pitch of the seed plate.

Figure 4 Structure of cell-wheel precision seed-metering device

Among them, the rotational speed of the seed-metering device fell within the range of 30.32-37.9 rpm. The driving motor and tachometers were used to realize the desired rotational speed of the device. The hole diameter range was 12-14 mm and the hole pitch range was 20.2-60.6 mm.

Seed plates with different hole diameters and hole pitches were tested. The test conditions are presented in Tab. 1.

Table 1 Test factors and codes

Code value	Rotational speed / X_1	Hole diameter / X_2	Hole pitch / X_3
1	37.9	14	60.6
0	34.11	13	40.4
−1	30.32	12	20.2

During the test, the first step involved clearing residual seeds from the seed-metering device, installing the required seed plate, and debugging the seed-metering device. Next, the high-speed camera was turned on and adjusted to a suitable angle so that seeds ejected from the holes of the seed plate could be clearly captured. Afterwards, the rotational speed of the seed-metering device was allowed to stabilize under the specified conditions. A sufficient number of seeds (100 was adopted as the standard for statistical analyses) were quickly added to the seed-metering device. Then, the high-speed camera was used to record the actual seed-metering process. Finally, the steps were repeated three times for each of the test conditions listed in Tab. 1.

Statistics were performed on the qualification, miss-seeding, and reseeding rate. In the initial stage, since seed filling is non-uniform, the actual seed-filling effect cannot be accurately reflected, therefore, the first 20 seeds ejected from the seed-metering device were excluded from the statistical analysis. Starting from 21, a total of 100 seeds were considered as one group of data. The test results are presented in Tab. 2.

Table 2 Test design and results

Trials	Coded level of variables			Experimental properties		
	X_1 / rpm	X_2 / rpm	X_3 / rpm	Y_1 / %	Y_2 / %	Y_3 / %
1	−1	−1	0	91.86	4.98	3.16
2	1	−1	0	86.29	9.30	4.41
3	−1	1	0	92.35	3.67	3.98
4	1	1	0	87.37	5.02	7.61
5	−1	0	−1	93.47	2.73	3.8
6	1	0	−1	87.62	6.59	5.79
7	−1	0	1	94.26	1.54	4.20
8	1	0	1	88.27	5.16	6.57
9	0	−1	−1	88.57	6.30	5.13
10	0	1	−1	87.12	5.22	7.66
11	0	−1	1	88.95	5.63	5.42
12	0	1	1	90.13	3.64	6.23
13	0	0	0	92.35	2.62	5.03
14	0	0	0	92.74	2.46	4.8
15	0	0	0	92.53	2.69	4.78
16	0	0	0	91.87	3.55	4.58
17	0	0	0	93.15	2.83	4.02

Note: ** high significant. * significant. n.s. not significant

3 RESULTS

Test data were analyzed and fitted using *Design-Expert (version 8.0.6)*. Regression equations were obtained for qualification index Y_1, miss-seeding index Y_2, and reseeding index Y_3 [26].

3.1 Regression Analysis of Qualification Index

A multiple regression analysis was performed on the test data to obtain regression models for various factors relative to the qualification index Y_1:

$$Y_1 = 92.53 - 2.8X_1 + 0.16X_2 + 0.6X_3 + 0.15X_1X_2 - 0.035X_1X_3 + 0.66X_2X_3 - 0.42X_1^2 - 2.64X_2^2 - 1.2X_3^2 \quad (9)$$

Tab. 3 shows results of the analysis of variance of qualification index Y_1. From Tab. 3, $P_{L1} = 0.3137 > 0.05$ indicating that no loss factor existed in the regression analysis, and the regression model exhibited a high fitting degree. The P-value of the model regression items, $P_{M1} < 0.0001 < 0.01$, indicated that the regression results were reliable to a certain extent. Among the interaction terms, X_1, X_2^2 and X_3^2 were highly significant terms, X_3 and X_2X_3 were significant terms. The model for qualified index was

regressed by considering only the significant terms and shown as:

$$Y_1 = 92.53 - 2.8X_1 + 0.6X_3 + 0.66X_2X_3 - -2.64X_2^2 - 1.2X_3^2 \quad (10)$$

Table 3 Analysis of variance

Source	Qualification Index / Y_1				Miss-seeding Index / Y_2				Reseeding Index / Y_3			
	SS	DF	F	P	SS	DF	F	P	SS	DF	F	P
Model	106.16	9	41.22	<0.0001**	59.04	9	23.68	0.0002**	25.14	9	14.49	0.0010**
X_1	62.66	1	219.00	<0.0001**	21.62	1	78.02	<0.0001**	10.67	1	55.35	0.0001**
X_2	0.21	1	0.74	0.4187 n. s.	9.37	1	33.84	0.0007**	6.77	1	35.12	0.0006**
X_3	2.92	1	10.19	0.0152*	2.96	1	10.70	0.0137*	0.0002	1	0.001	0.9752 n. s.
X_1X_2	0.087	1	0.30	0.5985 n. s.	2.21	1	7.96	0.0257*	1.42	1	7.34	0.0302*
X_1X_3	0.0049	1	0.017	0.8996 n. s.	0.014	1	0.052	0.8262 n. s.	0.036	1	0.19	0.6783 n. s.
X_2X_3	1.73	1	6.04	0.0436*	0.21	1	0.75	0.4160 n. s.	0.74	1	3.84	0.0910 n. s.
X_1^2	0.76	1	2.65	0.1479 n. s.	3.11	1	11.24	0.0122*	0.80	1	4.15	0.0810 n. s.
X_2^2	29.27	1	102.28	<0.0001**	17.74	1	64.02	<0.0001**	1.44	1	7.45	0.0294*
X_3^2	6.05	1	21.15	0.0025**	0.42	1	1.51	0.2591 n. s.	3.29	1	17.07	0.0044**
Residual	2.00	7			1.94	7			1.35	7		
Lack of fit	1.11	3	1.65	0.3137 n. s.	1.22	3	2.26	0.2232 n. s.	0.76	3	1.74	0.2965 n. s.
Error	0.90	4			0.72	4			0.59	4		
Total	108.16	16			60.98	16			26.49	16		

Note: ** highly significant (P < 0.01); * significant (0.01 < P < 0.05); n. s. not significant (P > 0..05)

3.2 Regression Analysis of Miss-Seeding Index

A multiple regression analysis was performed to obtain regression models of the various factors relative to miss-seeding index Y_2:

$$Y_2 = 2.83 + 1.64X_1 - 1.08X_2 - 0.61X_3 - 0.74X_1X_2 - 0.06X_1X_3 - 0.23X_2X_3 + 0.86X_1^2 + 2.05X_2^2 + 0.32X_3^2 \quad (11)$$

Tab. 3 shows results of the analysis of variance of miss-seeding index Y_2. From Tab. 3, $P_{L2} = 0.2232 > 0.05$, indicating that no loss factor existed in the regression analysis, and the regression model exhibited a high fitting degree. The P value of the model regression items, $P_{M2} = 0.0002 < 0.01$, indicated that the regression results were reliable to a certain extent. Among the interaction terms, X_1, X_2, and X_2^2 were highly significant terms, X_3, X_1X_2 and X_1^2 were significant terms. The model for miss-seeding index was regressed by considering only the significant terms and shown as:

$$Y_2 = 2.83 + 1.64X_1 - 1.08X_2 - 0.61X_3 - -0.74X_1X_2 + 0.86X_1^2 + 2.05X_2^2 \quad (12)$$

3.3 Regression Analysis of Reseeding Index

A multiple regression analysis was performed to obtain regression models of the various factors relative to reseeding index Y_3:

$$Y_3 = 4.64 + 1.16X_1 + 0.92X_2 + 0.005X_3 + 0.6X_1X_2 + +0.095X_1X_3 - 0.43X_2X_3 - 0.44X_1^2 + 0.58X_2^2 + 0.88X_3^2 \quad (13)$$

Tab. 5 shows results of the analysis of variance of reseeding index Y_3. From Tab. 5, $P_{L3} = 0.2965 > 0.05$ indicating that no loss factor existed in the regression analysis, and the regression model exhibited a high fitting degree. The P value of the model regression items, $P_{M3} = 0.001 < 0.01$ indicating that the regression results were reliable to a certain extent. Among the interaction terms,

X_1, X_2, and X_3^2 were highly significant terms, X_1X_2 and X_2^2 were significant terms. The model for reseeding index was regressed by considering only the significant terms and shown as:

$$Y_3 = 4.64 + 1.16X_1 + 0.92X_2 + 0.6X_1X_2 + +0.58X_2^2 + 0.88X_3^2 \quad (14)$$

3.4 Influence of Various Factors on the Test Indexes

The influence of experimental factors on the model is directly proportional to the value of contribution rate K, and the calculation method is as follows:

$$\theta = \begin{cases} 0 & F \le 1 \\ 1 - \dfrac{1}{F} & F > 1 \end{cases} \quad (15)$$

$$K_j = \theta_j + \frac{1}{2}\sum_{i=A}^{C}\theta_{ij} + \theta_j^2 \quad j = A, B, C \quad i \ne j \quad (16)$$

where, F is the F-value of each regression term in the regression equation; θ is the assessment value of the regression item to the F value; K_j is the contribution rate of each influencing factor.

According to Eq. (14), the contribution indices of rotational speed, hole diameter, hole pitch to the qualification index are 1.62, 1.41 and 2.27, the contribution of the factors to the qualification index followed the order as follows: hole pitch X_3 > rotational speed X_1 > hole diameter X_2; the contribution indices of rotational speed, hole diameter, hole pitch to the miss-seeding index are 2.34, 2.39 and 1.24, the contribution of the factors to the miss-seeding index followed the order as follows: hole diameter X_2 > rotational speed X_1 > hole pitch X_3; the contribution indices of rotational speed, hole diameter, hole pitch to the reseeding index are 2.17, 2.64 and 1.31, the contribution of the factors to the reseeding index followed the order as follows: hole diameter X_2 > rotational speed X_1 > hole pitch X_3.

3.5 Effects of Test Factors on Performance Indices

To express the interactive influence of each factor on the qualification index Y_1, miss-seeding index Y_2 and reseeding index Y_3, the above three quadratic regression equations of the evaluation indices were subjected to treatment. One of the factors was set to level 0, while the other two underwent interaction effect analysis (by removing the insignificant items: X_1X_2 and X_1X_3 in qualification index Y_1, X_1X_3 and X_2X_3 in miss-seeding index Y_2 and X_1X_3 and X_2X_3 in reseeding index Y_3) to study the influence law on the evaluation indices Y_1, Y_2 and Y_3, and the corresponding response surfaces were generated, as illustrated in Fig. 5.
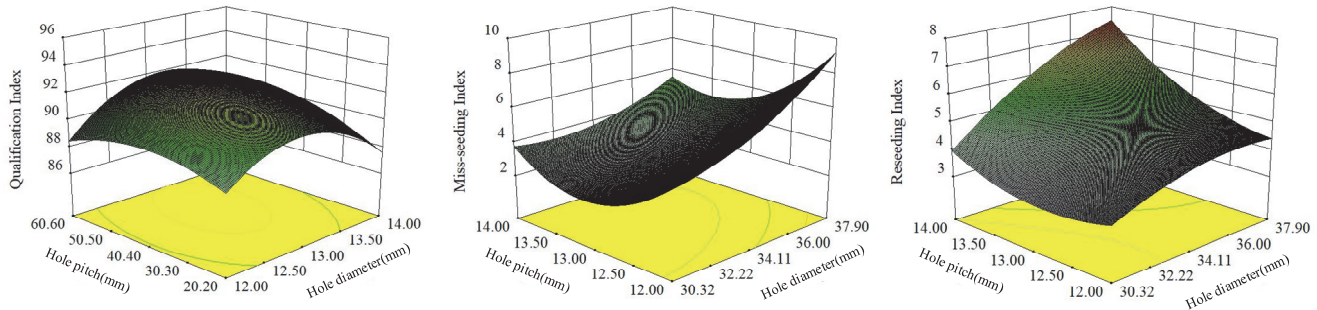

Figure 5 Effects of test factors on indices

Fig. 5a shows the effect of interaction between the hole diameter of the seed-metering device and hole pitch on the qualification index when the rotational speed of the seed-metering device is 34.11 rpm. For the given hole pitch, as the hole diameter increases, the qualification index first increases, then decreases. For the given hole diameter, as the hole pitch increases, the qualification index first increases, then decreases. Fig. 5b shows the effect of interaction between the rotational speed of the seed-metering device and the hole diameter on the miss-seeding index when the hole pitch is 40.4 mm. For the given hole diameter, as the rotational speed of the seed-metering device increases, the miss-seeding index gradually increases. At a constant rotational speed, as the hole diameter increases, the miss-seeding index first decreases, then increases. Fig. 5c shows the effect of interaction between the rotational speed of the seed-metering device and the hole diameter on reseeding index when the hole pitch is 40.4 mm. For the given hole diameter, as the rotational speed of the seed-metering device increases, the reseeding index gradually increases. For a constant rotational speed of the seed-metering device, as the hole diameter increases, the reseeding index gradually increases.

When the speed of the seed-metering device is low, the qualification index is better, because the seeds have enough time to enter the hole and complete the seed filling under the low-speed operation condition. However, as the speed of the seed-metering device increases, the seeds do not have enough time to enter the hole, resulting in increased miss-seeding index. On the other hand, the seeds rotate directly along the seed-metering wheel, leading to an increase in reseeding index. When the hole diameter is small, it is difficult for seeds to enter hole, which leads to lower qualification index and higher omission index. However, when the hole diameter is larger, the chance of seeds entering hole increases, and multiple seeds enter hole at the same time, which leads to the decline of qualified index and the increase of reseeding index. When the hole pitch is small, the time for seeds to enter holes is short, leading to a lower qualified index and

a higher miss-seeding index. However, with the increase of the hole pitch, the time for seeds to enter holes increases, leading to an increase in reseeding index.

3.6 Parameter Optimization

To identify the optimal combination of test factors levels, boundary conditions of the test factors and regression equations of the qualification index Y_1, the miss-seeding index Y_2 and the reseeding index Y_3 were combined to determine the optimal solution. The test indices were optimized for the maximum qualification index Y_1 and minimum miss-seeding index Y_2 and reseeding index Y_3.

$$\begin{cases} \max Y_1(X_1, X_2, X_3) \\ \min Y_2(X_1, X_2, X_3) \\ \min Y_3(X_1, X_2, X_3) \\ s.t. \begin{cases} 30.32 \text{ rpm} \le X_1 \le 37.9 \text{ rpm} \\ 12.00 \text{ mm} \le X_2 \le 14.00 \text{ mm} \\ 20.2 \text{ mm} \le X_3 \le 60.6 \text{ mm} \end{cases} \end{cases} \quad (17)$$

In the *Design-Expert* software, the optimal performance was achieved with a rotational speed of the seed-metering device of 30.32 rpm, hole diameter of 13 mm, and hole pitch of 45 mm; qualification rate, miss-seeding rate, and reseeding rate were 94.99%, 1.93%, and 3.08%, respectively.

3.7 Test Verification

To verify the optimized seeding performance parameters of the cell wheel seed-metering device for corn, seeding tests were carried out using *Zhengdan 958* corn seeds on an experimental plot in Yangling agricultural high-tech industries demonstration zone in mid-March 2021. The plot is characterized by flat terrain and fertile soil. The single-seed qualification index, reseeding index, and miss-seeding index were measured in accordance with the Testing methods of single seed drills (precision drills) (GB/T 6973-2005). The

field tests were carried out 5 times, and the detailed experimental data are shown in Tab. 4.

Table 4 Field test results

Number	Y_1 / %	Y_2 / %	Y_3 / %
1	92.20	2.76	5.04
2	89.45	4.30	6.25
3	93.68	2.34	3.98
4	91.40	3.42	5.18
5	92.32	2.58	5.10
$\bar{X}$	91.81	3.08	5.11

The field test results are the average values of 5 repeated tests, and show that the single-seed qualification index, miss-seeding index, and reseeding index are 91.81%, 3.08%, and 5.11%, respectively. Compared with the optimization results, the error rates of qualification index, miss-seeding index and reseeding index are 3.18%, 1.15% and 2.03%.

4 CONCLUSIONS

In this study, a cell wheel precision seed-metering device was designed and built. The following conclusions are drawn:

1) Through the test, the three test factors have an effect on the qualification index in the following order: hole pitch, rotational speed and hole diameter; at the same time, the hole diameter has the greatest influence on the miss-seeding index and reseeding index. Therefore, when designing a mechanical metering device, this can be used as a reference.

2) The results were fitted and optimized in the Design-expert data analysis software. The seed-metering device exhibited optimal performance under a rotational speed of the seed-metering device of 30.32 rpm, hole diameter of 13 mm, and hole pitch of 45 mm. The field test results showed that the qualification rate was 91.81%, the miss-seeding index was 3.08%, and the reseeding index was 5.11%. The field test results were consistent with the optimization results.

The device can realize the rapid detection of the performance of the seed-metering device, simplify the performance detection process of the seed-metering device, shorten the research and development cycle of the seed-metering device, and help promote the development of China's mechanical seed-metering device. However, only *Zhengdan 958* corn seeds were used to verify the experiment. Caution should be taken when using the other seeds.

Acknowledgement

5 REFERENCES

[1] Wang, J., Tang, H., Wang, J., Li, X., & Huang, H. (2017). Optimization design and experiment on ripple surface type pickup finger of precision maize seed metering device. *International Journal of Agricultural and Biological Engineering*, *10*(1),61-71. https://doi.org/10.3965/j.ijabe.20171001.2050

[2] Lv, X., Wang, X., Tian, Z., & Zhang, Z. (2020).Design of Automatic Reseeding System of Air Suction Precision Metering Seeding Device for Corn. *Mechatronic Systems and Control*, *48*(3), 152-158. https://doi.org/10.2316/J.2020.201-0038

[3] Liu, H., Guo, L., Fu, L., & Tang, S. (2015). Study on multi-size seed-metering device for vertical plate soybean precision planter. *International Journal of Agricultural and Biological Engineering*, *8*(1), 1-8. https://doi.org/10.3965/j.ijabe.20150801.001

[4] Anantachar, M., Kumar, G. V. P., & Guruswamy, T. (2011). Development of artificial neural network models for the performance prediction of an inclined plate seed metering device. *Applied Soft Computing*, *11*(4), 3753-3763. https://doi.org/10.1016/j.asoc.2011.02.006

[5] Yang, L., He, X., Cui, T., Zhang, D., Shi, S., Zhang, R., & Wang, M. (2015). Development of mechatronic driving system for seed meters equipped on conventional precision corn planter. *International Journal of Agricultural and Biological Engineering*, *8*(4), 1-9. https://doi.org/10.3965/j.ijabe.20150804.1717

[6] Yazgi, A. & Degirmencioglu, A. (2014). Measurement of seed spacing uniformity performance of a precision metering unit as function of the number of holes on vacuum plate. *Measurement*, *56*, 128-135. https://doi.org/10.1016/j.measurement.2014.06.026

[7] Qi, J., Jia, H., Li Yang., Yu, H., Liu, X., Lan, Y., Feng, X., & Yang, Y. (2015). Design and test offault monitoring system for corn precision planter. *International Journal of Agricultural & Biological Engineering*, *8*(6), 13-19. https://doi.org/10.3965/j.ijabe.20150806.1968

[8] Li, S., Gong, H., & Gu, H. (2010). Notice of retraction research on loss seeding monitoring and precise reseeding seeder system. *International Conference on Computer Application and System Modeling, IEEE*. https://doi.org/10.1109/ICCASM.2010.5619195

[9] Singh, T. & Mane, D. (2021). Development and Laboratory Performance of an Electronically Controlled Metering Mechanism for Okra Seed. *Agricultural Mechanization in Asia, Africa and Latin America*. *42*(2), 63-69.

[10] Yang, L., Yan, B., Cui, T., Yu, Y., He, X., Liu, Q., Liang, Z., Yin, X., & Zhang, D. (2016). Global overview of research progress and development of precision maize planters. *International Journal of Agricultural and Biological Engineering, 9*(1), 9-26. https://doi.org/10.3965/j.ijabe.20160901.2285

[11] Mao, X., Yi, S., Tao, G., Yang L., Liu, H., & Ma, Y. (2015). Experimental study on seed-filling performance of maize bowl-tray precision seeder. *International Journal of Agricultural and Biological Engineering, 8*(2), 31-38. https://doi.org/10.3965/j.ijabe.20150802.1809

[12] St Jack, D., Hesterman, D. C., & Guzzomi, A. L. (2013). Precision metering of Santalum spicatum (Australian Sandalwood) seeds. *Biosystems Engineering, 115*(2), 171-183. https://doi.org/10.1016/j.biosystemseng.2013.03.004

[13] Chen, W., Zhang, B., Jiang, L., Qiu, T., Wang, L., & Yang, S. (2020). Research status and development trend of seed-metering device in China. *American Journal of Agricultural Research*, *5*.

[14] Zhang, J., Li, Z., Liu, H., & Wu, G. (2016). Mathematical modeling and validation of seeder's suction-boundary on pneumatic-roller type metering. *Transactions of the Chinese Society of Agricultural Engineering*, *32*(23), 12-20. https://doi.org/10.11975/j.issn.1002-6819.2016.23.002

[15] Gao, X., Cui, T., Zhou, Z., Yu, Y., Xu, Y., Zhang, D., & Song, W. (2021). DEM study of particle motion in novel high-speed seed metering device. *Advanced Powder Technology, 32*(5),1438-1449. https://doi.org/10.1016/j.apt.2021.03.002

[16] Woo, S. M., Uyeh, D. D., Sagong, M. S., & Ha, Y. S. (2017). Development of seeder for mixed planting of corn and

soybeans. *International Journal of Agricultural and Biological Engineering*, *10*(3), 95-101.
https://doi.org/10.3965/j.ijabe.20171003.2543

[17] Lei, X., Liao, Y., Zhang, Q., Wang, L., & Liao, Q. (2018). Numerical simulation of seed motion characte-ristics of distribution head for rapeseed and wheat. *Computers and Electronics in Agriculture*, *150*, 98-109.
https://doi.org/10.1016/j.compag.2018.04.009

[18] Lei, X., Liao, Y., & Liao, Q. (2016). Simulation of seed motion in seed feeding device with DEM-CFD coupling approach for rapeseed and wheat. *Computers and Electronics in Agriculture*, *131*, 29-39.
https://doi.org/10.1016/j.compag.2016.11.006

[19] Du, X., Liu, C., Jiang, M., Zhang, F., Yuan, H., & Yang, H. (2019). Design and experiment of self-disturbance inner-filling cell wheel maize precision seed-metering device. *Transactions of the Chinese Society of Agricultural Engineering, 35*(13), 23-34.
https://doi.org/10.11975/j.issn.1002-6819.2019.13.003

[20] Zhang, D., He, J., Li, H., Wang, T., Zhang, X., Zheng, Z., Lu, Z., & Wang, S. (2013). Design and experiment on double cam-link of continuously variable transmission for seeding and fertilizing. *Transactions of the Chinese Society of Agricultural Engineering*, *29*(10), 9-17.
https://doi.org/10.3969/j.issn.1002-6819.2013.09.002

[21] Lu, Z., Li, Z., & Zhao, C. (2019). A Novel Method for Reconstructing Flatness Error Contour of Long Surface Based on a Laser Displacement Sensor. *IEEE Access*, *7*, 118088-118100. https://doi.org/10.1109/access.2019.2936445

[22] Pereira, F., Sampaio, H., Chaves, R., Correia, R., Luis, M., Sargento, S., Jordao, M., Almeida, L., Senna, C., Oliveira, A. S. R., & Carvalho, N. B. (2020). When Backscatter Communication Meets Vehicular Networks: Boosting Crosswalk Awareness. *IEEE Access*, *8*, 34507-34521.
https://doi.org/10.1109/access.2020.2974214

[23] Athijayamani, A., Ganesamoorthy, R., Loganathan, K. T., & Sidhardhan, S. (2016). Modelling and Analysis of the Mechanical Properties of Agave Sisalana Variegata Fibre/Vinyl Ester Composites Using Box-Behnken Design of Response Surface Methodology. *Strojniski Vestnik - Journal of Mechanical Engineering*, *62*(5), 273-280.
https://doi.org/10.5545/sv-jme.2015.2641

[24] Yin, X., Noguchi, N., Yang, T. X., & Jin, C. Q. (2018). Development and evaluation of a low-cost precision seeding control system for a corn drill. *International Journal of Agricultural and Biological Engineering*, *11*(5), 95-99. https://doi.org/10.25165/j.ijabe.20181105.3369

[25] Han, D., Zhang, D., Jing, H., Yang, L., Cui, T., Ding, Y., Wang, Z., Wang, Y., & Zhang, T. (2018). DEM-CFD coupling simulation and optimization of an inside-filling air-blowing maize precision seed-metering device. *Computers and Electronics in Agriculture*, *150*, 426-438.
https://doi.org/10.1016/j.compag.2018.05.006

[26] Grguras, D. & Kramar, D. (2017). Optimization of Hybrid Manufacturing for Surface Quality, Material Consumption and Productivity Improvement. *Strojniski Vestnik - Journal of Mechanical Engineering*, *63*(10), 567-576.
https://doi.org/10.5545/sv-jme.2017.4396

Contact information:

Kezhou CHEN, Graduate Student
College of Mechanical and Electronic Engineering, Northwest A&F University,
Yangling, Shaanxi 712100, China
E-mail: ckz@nwafu.edu.cn

Xing LIU, Graduate Student
College of Mechanical and Electronic Engineering, Northwest A&F University,
Yangling, Shaanxi 712100, China
E-mail: xingliu_hn@163.com

Xin HE, Graduate Student
College of Mechanical and Electronic Engineering, Northwest A&F University,
Yangling, Shaanxi 712100, China
E-mail: hexinnwafu@163.com

Xun WANG, Graduate Student
College of Mechanical and Electronic Engineering, Northwest A&F University,
Yangling, Shaanxi 712100, China
E-mail: wwccandlks@163.com

Yanzhi LIU, Engineer
SHAANXI LEOPARD SUSPENSION SYSTEMS LTD,
Baoji, Shaanxi 722200, China
E-mail: 1010924401@qq.com

Wei LI, PhD, Associate Professor
(Corresponding author)
College of Mechanical and Electronic Engineering, Northwest A&F University,
Yangling, Shaanxi 712100, China
E-mail: liweizibo@nwsuaf.edu.cn